

Literatur

- BUSING, W. R., MARTIN, K. O. & LEVY, H. A. (1962). ORNL-TM-305, Oak Ridge National Laboratory, Oak Ridge, Tennessee.
- BUSING, W. R., MARTIN, K. O. & LEVY, H. A. (1964). ORNL-TM-306, Oak Ridge National Laboratory, Oak Ridge, Tennessee.
- CHASTAIN, R. V. (1965). Least-squares Line and Plane Program in 'X-ray 63', Dept. Chem., Univ. Washington and Univ. Maryland.
- ECK, J. (1970). Unveröffentlichtes Programm.
- ECK, J. & RIECHERT, L. (1970). *J. Appl. Cryst.* **3**, 332.
- HANSON, H. P., HERMAN, F., LEA, J. D. & SKILLMAN, S. (1964). *Acta Cryst.* **17**, 1040.
- JOHNSON, C. K. (1965). ORNL-3794, Revised, Oak Ridge National Laboratory, Oak Ridge, Tennessee.
- KARLE, J. & KARLE, I. L. (1966). *Acta Cryst.* **21**, 849.
- KRAEFT, U. (1966). Unveröffentlichtes Programm.
- PERDOK, W. G. & TERPSTRA, P. (1943). *Rec. Trav. chim. Pays-Bas*, **62**, 687.
- PERDOK, W. G. & TERPSTRA, P. (1946). *Rec. Trav. chim. Pays-Bas*, **65**, 493.
- STEWART, R. F., DAVIDSON, E. R. & SIMPSON, W. T. (1965). *J. Chem. Phys.* **42**, 3175.

Acta Cryst. (1972). **B28**, 610

The Crystal Structure of 11-Bromoundecanol

BY LAWRENCE ROSEN* AND ALBERT HYBL

Department of Biophysics, University of Maryland School of Medicine, Baltimore, Maryland 21201, U.S.A.

(Received 7 January 1971 and in revised form 3 May 1971)

The crystal structure of 11-bromoundecanol ($C_{11}H_{23}BrO$) was determined by heavy-atom methods. This alcohol crystallizes from ethyl acetate, showing a tabular monoclinic aspect having space group $P2_1$ with $a=47.10$ (8), $b=5.26$ (1), $c=31.14$ (6) Å, $\beta=132.9$ (2)° and $Z=18$; $D_m=1.347$ g.cm $^{-3}$. Three-dimensional data, gathered with a G.E. manual diffractometer using Ni-filtered Cu $K\alpha$ ($\lambda=1.5418$), show a very prominent subcell with $Z=2$, having dimensions $a=5.23$, $b=5.26$, $c=22.81$ Å, and $\beta=90.6^\circ$. The arrangement of molecules in both the true unit cell and the subcell was determined and refined by block-diagonal least-squares ($R=0.14$) methods. The van der Waals attractions between planes of bromine atoms appear to dictate the packing preference for the large cell over the subcell, and may account for the 23° rise in melting point when compared to dodecanol. The hydrocarbon chain packing is the triclinic parallel type.

Introduction

The crystal structure of 11-bromoundecanol, $Br[CH_2]_{11}OH$, hereafter referred to as BUOL, has been investigated as part of a series of lipid compounds being studied in our laboratory. Very little single-crystal work on long-chain alcohols has been reported. Almost all X-ray crystallographic studies in this area have been carried out on microcrystalline powders (Tanaka, Seto & Hayashida, 1957; Tanaka, Seto, Watanabe & Hayashida, 1959; Watanabe, 1961, 1962; Malkin, 1930; Kolb & Lutton, 1951). These investigations clarified the relationship between polymorphic thermal behavior and molecular tilt. Single-crystal work has been essentially limited to projection studies (Welsh, 1956, 1960; Abrahamsson, Larsson & von Sydow, 1960).

BUOL molecules pack in an unusual manner. There are 18 molecules in a monoclinic cell. A well-defined subcell also exists within the intensity-weighted recip-

rocal lattice of the true cell. This smaller cell contains two molecules of BUOL.

The structures of both cells were solved in the hope that differences between them could be used to explain why the larger cell was favored over the simpler arrangement of the subcell.

Experimental

BUOL was prepared from recrystallized commercial grade 11-bromoundecanoic acid by a $LiAlH_4$ reduction of its freshly prepared and fractionally distilled acid chloride. The product was purified by vacuum distillation, and recrystallized several times from ethyl acetate or phenyl bromide producing tabular crystals suitable for X-ray work. The crystals are easily deformed and cleave parallel to their long direction. They show polymorphic melting behavior: low-melting form at 39–40°C, and a high-melting form at 46°C.

Oscillation and Weissenberg films about the long axis of a BUOL crystal showed $2/m$ Laue symmetry with the b axis coincident with the spindle direction. Some crystals showed pseudo-merohedral twinning. A

* Present address: Department of Biochemistry, Columbia University, College of Physicians and Surgeons, 630 West 168th Street, New York, New York 10032, U.S.A.

diffractometer scan of the $0k0$ reflections showed only the presence of the 020 reflection. Because of the limited diffraction in this direction there was some doubt as to the choice of space group. A successful refinement was made using $P2_1$. Physical constants for BUOL are listed in Table 1. The festoons having h indices of zero or multiples of nine ($00l$, $90l$, $180l$, etc.) contain practically all observed reflections of the $h0l$ layer. This defines a subcell within the larger true cell with the dimensions given in Table 1. Both cells share a common b axis. A drawing of the $h0l$ intensity-weighted reciprocal lattice net is shown in Fig. 1.

Table 1. *Physical constants of BUOL*

M.F.	$\text{BrC}_{11}\text{H}_{23}\text{O}$		
M.W.	261.2 g./mole		
Melting point	39 to 46.2°C		
Habit	Elongated parallelepipeds		
D_x	1.347 g./cm ³		
D_m	1.327 g./cm ³		
Radiation	Cu $K\alpha$ (1.5418 Å)		
Crystal size (average)	0.25 × 0.4 × 0.06 mm		
μ	44.7 cm ⁻¹		
	True cell	Subcell	Methylene subcell
a	47.10 (8) Å	5.23 Å	4.50 (9) Å
b	5.26 (1)	5.26	5.26 (0)
c	31.14 (6)	22.81	2.52 (4)
α	90.0°	90.0°	64 (2)°
β	132.9 (2)	90.6	114 (1)
γ	90.0	90.0	118 (1)
Systematic absences	$0k0$ for $k=2n+1$	$0k0$ for $k=2n+1$	—
Space group	$P2_1$	$P2_1$	$T_1 - P\bar{1}$
Z	18	2	2-CH ₂ -units
V	5651.4 Å ³	627.9 Å ³	45.6 (8) Å ³
Total independent reflections	12280	1365	—
Total observed reflections	1353	456	—

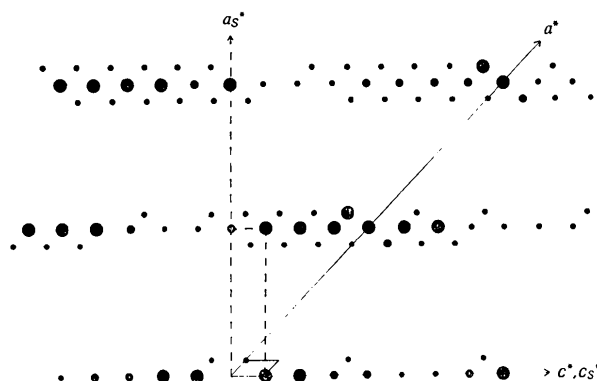


Fig. 1. The intensity-weighted reciprocal lattice of 11-bromo-undecanol. The subcell is drawn with dashed lines and subscripted axes.

The relative dominance of festoons whose h indices are multiples of nine disappears with increasing k index. Weissenberg films of the $h2l$ and $h3l$ layers show clusters of five festoons where $h=9n$, $9n\pm 1$, and $9n\pm 2$ with $n=0, 1, 2, \dots$, and in which intensities of the $h=9n$ festoons are not noticeably greater than their two nearest neighbors. Therefore, differences among the nine molecules of the asymmetric unit are primarily related to variations in their y coordinates. Since the $h0l$ layer consisted almost entirely of subcell reflections, it can be inferred that the x and z coordinates of the nine BUOL molecules closely follow the symmetry requirements of the subcell.

Due to rapid crystal decay, four crystals were required to collect a complete set of intensity data, one for each layer of k index 0 to 3. An ($h0l$) Weissenberg photograph of each data crystal was taken to eliminate twinned crystals and crystals of poor quality. Peak intensities were measured by the stationary-crystal stationary-counter method on a manual G.E. diffractometer.

To minimize crystal decay, Weissenberg films were used as a guide in collecting data. Extensive regions of reciprocal space that were devoid of observable intensities were not measured. However, a small number of reflections considered unobserved on film were measured to determine if the film had been exposed long enough to record all of the observable diffraction pattern. Without exception, reflections not observed on film exhibited no net intensity when they were measured.

While Weissenberg films and visual criteria were used to distinguish between observed and unobserved festoons, all festoons that were designated observed by these standards contained weak or doubtful reflections. The following relationship was used to determine if an individual reflection was to be designated observed: $C_p - C_b > 3(C_p)^{1/2}$, where C_p and C_b represent the total peak and background counts, respectively. Peak counts not obeying this inequality were designated unobserved.

Every peak position was counted for 40 sec and a 20-sec background count was taken at $\Delta 2\theta = -1.67^\circ$. Intensities used in data reduction were set equal to the peak-height count, less twice the background count, and then converted to the corresponding integrated intensities by the method of Alexander & Smith (1962).

Four standard reflections were monitored for intensity decay at intervals of 50 reflections during data collection. Another group of 75 reflections was measured for each of the four BUOL crystals to provide inter-layer scaling constants. Data from each crystal were first corrected for intensity decline. The fractional intensity decline per observation ranged between 0.0002 to 0.0010 with the average at about 0.0007. The data were then scaled together using the procedure outlined in Table 2. Finally, intensities were corrected for Lorentz polarization effects and reduced to structure-factor amplitudes.

Table 2. *Scaling procedure*

Data from each crystal were first corrected for intensity decay. The ratio $S_j = \sum [F_o(hkl)] / \sum F_o(hkl)_j$ was calculated for each layer j using the 75 scaling reflections. The scaling ratios were independent of intensity, and the standard deviation of individual ratios was 6 to 8 %.

Crystal j	Layer	S_j	Number of measured reflections
1	$h0l$	1.000	353
2	$h1l$	0.881	406
3	$h2l$	1.661	392
4	$h3l$	1.426	202

The X-ray scattering curves used were for neutral atoms (*International Tables for X-ray Crystallography* 1962) with the bromine curve corrected for the anomalous dispersion term $\Delta f' = -0.9e$ (*International Tables* 1962). The term $\Delta f'' = 1.4e$ was neglected. The Aikens method with four differences was used for interpolating between tabulated values. Unfortunately, accurate dimensions of the four data crystals were not measured, which precluded making absorption corrections.

Molecular drawings were made with program ORTEP (Johnson, 1965).

Structure determination

Subcell refinement

The x and z coordinates of the two subcell bromine atoms were obtained from an $h0l$ Patterson projection. The set of subcell structure factors used in its calculation was extracted from the data set of the true cell by the matrix given below. Only those reflections having integer h' , k' , l' indices were included in the subcell data set.

$$\begin{pmatrix} \frac{1}{9} & 0 & 0 \\ 0 & 1 & 0 \\ \frac{4}{9} & 0 & 1 \end{pmatrix} \begin{pmatrix} h \\ k \\ l \end{pmatrix} = \begin{pmatrix} h' \\ k' \\ l' \end{pmatrix}$$

The phases determined by these bromine coordinates in an $h0l$ electron-density calculation were sufficiently correct to show all the non hydrogen atoms of each BUOL molecule. The observed foreshortening of the BUOL molecules in this projection was consistent with an extended aliphatic chain tilted some 26° with respect to the ac plane of the subcell. The addition of light-

atom positional and thermal parameters to least-squares refinement reduced R to its final value of 0.09.

It was possible to calculate a set of y coordinates for the subcell molecules solely from considering molecular tilt and the use of expected bond distances and angles.

The R value associated with the initial three-dimensional model was 0.22. Ten cycles of block-diagonal least-squares refinement lowered this value to 0.09 for the full set of 456 subcell reflections. No attempts were made to locate hydrogen atoms. The positional and thermal parameters produced by the last cycle of refinement are given in Tables 3 and 4.

Table 3. *Fractional atomic coordinates of the BUOL subcell molecule*

Coordinates listed below are multiplied by 10^4 . E.s.d.'s are given in parentheses and refer to the last decimal positions of their respective values.

	x/a	y/b	z/c
Br	3484 (05)	0 (0)	452 (01)
C(11)	2021 (53)	3502 (46)	723 (12)
C(10)	231 (47)	2959 (59)	1263 (11)
C(9)	9028 (37)	5426 (60)	1433 (09)
C(8)	7261 (39)	4653 (68)	1968 (10)
C(7)	6116 (41)	7262 (66)	2152 (10)
C(6)	4338 (44)	6953 (55)	2720 (11)
C(5)	3155 (41)	9377 (52)	2889 (10)
C(4)	1492 (47)	9116 (45)	3439 (12)
C(3)	397 (52)	1280 (46)	3646 (13)
C(2)	8587 (54)	1051 (43)	4178 (13)
C(1)	7502 (54)	3693 (47)	4353 (13)
O	5813 (31)	3348 (32)	4847 (08)

Refinement in the true cell

A three-dimensional Patterson map, generated with the full set of true-cell data, exhibited a nearly linear array of eight bromine-bromine vector peaks, approximately coincident with the a axis of the large cell. While these peaks lay essentially in the ac plane, there were some significant deviations from the ac plane as shown in Fig. 2. These peaks were about 5.2 \AA apart, which agreed closely with the symmetry requirements of the subcell whose axial repeat in this direction is 5.26 \AA . One trial model immediately suggested by this Patterson map was an inverted 'V' pointing in the b direction. The vertex of this model is occupied by the fifth bromine atom in an array of nine.

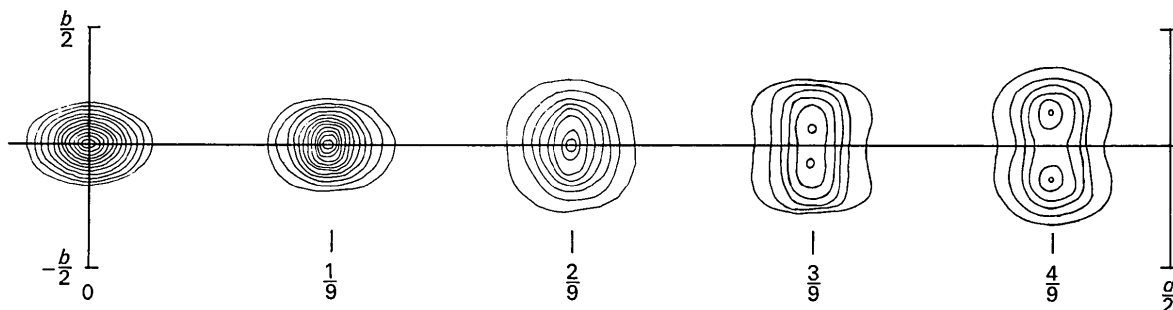


Fig. 2 The (UVO) section of the three-dimensional Patterson map of 11-bromoundecanol showing the Br-Br vector deviation from the ac plane.

Four cycles of positional and isotropic thermal refinement of these nine bromine atoms resulted in an R value of 0.26. The electron-density map phased by

these atoms contained peaks corresponding to more than 90 of the remaining 108 light atoms. When these were used to calculate subsequent Fourier maps, all

Table 4. *Final anisotropic thermal parameters of BUOL subcell atoms*

E.s.d.'s are in parentheses. All anisotropic values are multiplied by 10^4 and are defined by the expression:

$$\exp [-(B_{11}h^2 + B_{22}k^2 + B_{33}l^2 + B_{12}hk + B_{13}hl + B_{23}kl)]$$

	B_{11}	B_{22}	B_{33}	B_{12}	B_{13}	B_{23}
Br	810 (14)	1177 (18)	40 (1)	-115 (8)	180 (8)	-4 (14)
C(11)	774 (155)	1041 (226)	27 (7)	-131 (108)	134 (105)	6 (52)
C(10)	746 (141)	649 (164)	34 (7)	26 (167)	24 (162)	85 (60)
C(9)	613 (106)	522 (139)	34 (6)	-144 (70)	134 (66)	8 (64)
C(8)	673 (115)	647 (137)	34 (6)	-124 (76)	128 (70)	35 (70)
C(7)	631 (126)	668 (161)	30 (7)	-134 (223)	129 (224)	8 (61)
C(6)	660 (130)	419 (131)	37 (7)	-81 (134)	106 (130)	-4 (47)
C(5)	616 (122)	786 (192)	33 (7)	-120 (76)	107 (69)	58 (54)
C(4)	702 (139)	860 (225)	39 (8)	-65 (92)	136 (84)	-59 (46)
C(3)	689 (155)	828 (264)	38 (9)	180 (122)	25 (106)	-50 (46)
C(2)	761 (147)	867 (237)	38 (8)	-31 (103)	156 (90)	-4 (43)
C(1)	700 (144)	1026 (272)	32 (8)	-44 (99)	134 (93)	-8 (45)
O	690 (102)	811 (131)	38 (5)	-78 (80)	149 (77)	34 (28)

Table 5. *Observed structure factors*

The two columns contain values of I and $10|F_o|$.

hkl	I	$10 F_o $	hkl	I	$10 F_o $	hkl	I	$10 F_o $	hkl	I	$10 F_o $
0 0 0	1000	1000	1 1 1	100	100	2 2 2	100	100	3 3 3	100	100
1 1 1	100	100	2 2 2	100	100	3 3 3	100	100	4 4 4	100	100
2 2 2	100	100	3 3 3	100	100	4 4 4	100	100	5 5 5	100	100
3 3 3	100	100	4 4 4	100	100	5 5 5	100	100	6 6 6	100	100
4 4 4	100	100	5 5 5	100	100	6 6 6	100	100	7 7 7	100	100
5 5 5	100	100	6 6 6	100	100	7 7 7	100	100	8 8 8	100	100
6 6 6	100	100	7 7 7	100	100	8 8 8	100	100	9 9 9	100	100
7 7 7	100	100	8 8 8	100	100	9 9 9	100	100	10 10 10	100	100
8 8 8	100	100	9 9 9	100	100	10 10 10	100	100	11 11 11	100	100
9 9 9	100	100	10 10 10	100	100	11 11 11	100	100	12 12 12	100	100
10 10 10	100	100	11 11 11	100	100	12 12 12	100	100	13 13 13	100	100
11 11 11	100	100	12 12 12	100	100	13 13 13	100	100	14 14 14	100	100
12 12 12	100	100	13 13 13	100	100	14 14 14	100	100	15 15 15	100	100
13 13 13	100	100	14 14 14	100	100	15 15 15	100	100	16 16 16	100	100
14 14 14	100	100	15 15 15	100	100	16 16 16	100	100	17 17 17	100	100
15 15 15	100	100	16 16 16	100	100	17 17 17	100	100	18 18 18	100	100
16 16 16	100	100	17 17 17	100	100	18 18 18	100	100	19 19 19	100	100
17 17 17	100	100	18 18 18	100	100	19 19 19	100	100	20 20 20	100	100
18 18 18	100	100	19 19 19	100	100	20 20 20	100	100	21 21 21	100	100
19 19 19	100	100	20 20 20	100	100	21 21 21	100	100	22 22 22	100	100
20 20 20	100	100	21 21 21	100	100	22 22 22	100	100	23 23 23	100	100
21 21 21	100	100	22 22 22	100	100	23 23 23	100	100	24 24 24	100	100
22 22 22	100	100	23 23 23	100	100	24 24 24	100	100	25 25 25	100	100
23 23 23	100	100	24 24 24	100	100	25 25 25	100	100	26 26 26	100	100
24 24 24	100	100	25 25 25	100	100	26 26 26	100	100	27 27 27	100	100
25 25 25	100	100	26 26 26	100	100	27 27 27	100	100	28 28 28	100	100
26 26 26	100	100	27 27 27	100	100	28 28 28	100	100	29 29 29	100	100
27 27 27	100	100	28 28 28	100	100	29 29 29	100	100	30 30 30	100	100
28 28 28	100	100	29 29 29	100	100	30 30 30	100	100	31 31 31	100	100
29 29 29	100	100	30 30 30	100	100	31 31 31	100	100	32 32 32	100	100
30 30 30	100	100	31 31 31	100	100	32 32 32	100	100	33 33 33	100	100
31 31 31	100	100	32 32 32	100	100	33 33 33	100	100	34 34 34	100	100
32 32 32	100	100	33 33 33	100	100	34 34 34	100	100	35 35 35	100	100
33 33 33	100	100	34 34 34	100	100	35 35 35	100	100	36 36 36	100	100
34 34 34	100	100	35 35 35	100	100	36 36 36	100	100	37 37 37	100	100
35 35 35	100	100	36 36 36	100	100	37 37 37	100	100	38 38 38	100	100
36 36 36	100	100	37 37 37	100	100	38 38 38	100	100	39 39 39	100	100
37 37 37	100	100	38 38 38	100	100	39 39 39	100	100	40 40 40	100	100
38 38 38	100	100	39 39 39	100	100	40 40 40	100	100	41 41 41	100	100
39 39 39	100	100	40 40 40	100	100	41 41 41	100	100	42 42 42	100	100
40 40 40	100	100	41 41 41	100	100	42 42 42	100	100	43 43 43	100	100
41 41 41	100	100	42 42 42	100	100	43 43 43	100	100	44 44 44	100	100
42 42 42	100	100	43 43 43	100	100	44 44 44	100	100	45 45 45	100	100
43 43 43	100	100	44 44 44	100	100	45 45 45	100	100	46 46 46	100	100
44 44 44	100	100	45 45 45	100	100	46 46 46	100	100	47 47 47	100	100
45 45 45	100	100	46 46 46	100	100	47 47 47	100	100	48 48 48	100	100
46 46 46	100	100	47 47 47	100	100	48 48 48	100	100	49 49 49	100	100
47 47 47	100	100	48 48 48	100	100	49 49 49	100	100	50 50 50	100	100
48 48 48	100	100	49 49 49	100	100	50 50 50	100	100	51 51 51	100	100
49 49 49	100	100	50 50 50	100	100	51 51 51	100	100	52 52 52	100	100
50 50 50	100	100	51 51 51	100	100	52 52 52	100	100	53 53 53	100	100
51 51 51	100	100	52 52 52	100	100	53 53 53	100	100	54 54 54	100	100
52 52 52	100	100	53 53 53	100	100	54 54 54	100	100	55 55 55	100	100
53 53 53	100	100	54 54 54	100	100	55 55 55	100	100	56 56 56	100	100
54 54 54	100	100	55 55 55	100	100	56 56 56	100	100	57 57 57	100	100
55 55 55	100	100	56 56 56	100	100	57 57 57	100	100	58 58 58	100	100
56 56 56	100	100	57 57 57	100	100	58 58 58	100	100	59 59 59	100	100
57 57 57	100	100	58 58 58	100	100	59 59 59	100	100	60 60 60	100	100
58 58 58	100	100	59 59 59	100	100	60 60 60	100	100	61 61 61	100	100
59 59 59	100	100	60 60 60	100	100	61 61 61	100	100	62 62 62	100	100
60 60 60	100	100	61 61 61	100	100	62 62 62	100	100	63 63 63	100	100
61 61 61	100	100	62 62 62	100	100	63 63 63	100	100	64 64 64	100	100
62 62 62	100	100	63 63 63	100	100	64 64 64	100	100	65 65 65	100	100
63 63 63	100	100	64 64 64	100	100	65 65 65	100	100	66 66 66	100	100
64 64 64	100	100	65 65 65	100	100	66 66 66	100	100	67 67 67	100	100
65 65 65	100	100	66 66 66	100	100	67 67 67	100	100	68 68 68	100	100
66 66 66	100	100	67 67 67	100	100	68 68 68	100	100	69 69 69	100	100
67 67 67	100	100	68 68 68	100	100	69 69 69	100	100	70 70 70	100	100
68 68 68	100	100	69 69 69	100	100	70 70 70	100	100	71 71 71	100	100
69 69 69	100	100	70 70 70	100	100	71 71 71	100	100	72 72 72	100	100
70 70 70	100	100	71 71 71	100	100	72 72 72	100	100	73 73 73	100	100
71 71 71	100	100	72 72 72	100	100	73 73 73	100	100	74 74 74	100	100
72 72 72	100	100	73 73 73	100	100	74 74 74	100	100	75 75 75	100	100
73 73 73	100	100	74 74 74	100	100	75 75 75	100	100	76 76 76	100	100
74 74 74	100	100	75 75 75	100	100	76 76 76	100	100	77 77 77	100	100
75 75 75	100	100	76 76 76	100	100	77 77 77	100	100	78 78 78	100	100
76 76 76	100	100	77 77 77	100	100	78 78 78	100	100	79 79 79	100	100
77 77 77	100	100	78 78 78	100	100	79 79 79	100	100	80 80 80	100	100
78 78 78	100	100	79 79 79	100	100	80 80 80	100	100	81 81 81	100	100
79 79 79	100	100	80 80 80	100	100	81 81 81	100	100	82 82 82	100	100
80 80 80	100	100	81 81 81	100	100	82 82 82	100	100	83 83 83	100	100
81 81 81	100	100	82 82 82	100	100	83 83 83	100	100	84 84 84	100	100
82 82 82	100	100	83 83 83	100	100	84 84 84	100	100	85 85 85	100	100
83 83 83	100	100	84 84 84	100	100	85 85 85	100	100	86 86 86	100	100
84 84 84	100	100	85 85 85	100	100	86 86 86	100	100	87 87 87	100	100
85 85 85	100	100	86 86 86	100	100	87 87 87	100	100	88 88 88	100	100
86 86 86	100	100	87 87 87	100	100	88 88 88	100	100	89 89 89	100	100
87 87 87	100	100	88 88 88	100	100	89 89 89	100	100	90 90 90	100	100

108 light-atom positions were identified. The residual for all 117 non hydrogen atoms was 0.22.

Despite this progress, least-squares refinement could not produce any further improvement in the residual. Parameter shifts were apparently insufficiently constrained by the data. While each of the nine BUOL molecules of the asymmetric unit maintained its position relative to its neighbors, individual atoms tended to distribute themselves in regions incompatible with a well-defined subcell.

Because of the presence of the subcell, there were many more unobserved than observed reflections within the limit of the data. These unobserved reflections contain as much information as very strong reflections, since the presence of a weak reflection is just as unlikely an occurrence as a strong one (Stout & Jensen, 1968).

With this consideration in mind, 3800 unobserved reflections within the limit of the data were assigned values of $F_{\min}/2$ and were included in the refinement. The initial R value of 0.63 was rapidly reduced to 0.20 by the use of anisotropic thermal parameters for bromine alone, and isotropic thermal parameters for carbon and oxygen. The residual for observed reflections alone was 0.142. During refinement, unobserved reflections whose calculated structure-factor amplitudes were less than the $F_{\min}/2$ value assigned them were given zero weight; otherwise, the weight used was the average value calculated for several borderline observed reflections. Observed reflections were assigned a weight w , where $w = 1/\sigma(F^2)$ and

$$\sigma(F^2) = \frac{1}{L_p} \{C_p + C_b + [0.05 (C_p - C_b)]^2 + (0.05 C_b)^2\}^{1/2}.$$

In addition, the quantity $S = [\sum w^2 (|F_o|^2 - |F_c|^2)^2 / (n-p)]^{1/2}$, where n = the number of reflections and p the number of parameters in refinement, was monitored throughout the refinement. Observed reflections whose

ratios $(F_o^2 - F_c^2)/\sigma(F^2)$ exceeded $3S$ were also given zero weight during least-squares refinement. Table 5 gives a listing of observed structure factors. A complete listing of observed and calculated structure factors is available on request from A.H. Final positional and thermal parameters for the true cell are given in Tables 6 and 7.

Table 6. *Fractional atomic coordinates of the nine bromine atoms of the asymmetric unit of the BUOL true cell*

Coordinates are multiplied by 10^4 with e.s.d.'s given in parentheses. The atom numbering in the first column refers to different molecules. A complete listing of carbon and oxygen position coordinates is available upon request from one of the authors (A.H.). Their positions are adequately represented by a translation of the subcell parameters to place the Br atom in coincidence with the true cell Br positions.

	X/a	Y/b	Z/c
Br(1)	593 (5)	-196 (23)	445 (8)
2	1643 (5)	246 (26)	399 (8)
3	2727 (5)	797 (24)	366 (7)
4	3864 (4)	1391 (25)	390 (6)
5	5052 (5)	1644 (20)	452 (8)
6	3816 (5)	6335 (24)	9516 (7)
7	2686 (5)	5790 (23)	9496 (7)
8	1567 (4)	5376 (24)	9486 (6)
9	484 (4)	4770 (22)	9534 (6)

Attempts to refine anisotropic carbon and oxygen thermal parameters lowered R to 0.125 for the class of observed reflections only. However, thermal ellipsoids that resulted were often of an extremely elongated and/or flattened appearance, and the improvement in R was rejected as physically meaningless. A second reason for rejecting the improvement in R was based on the work of Hamilton (1965) who demonstrated that a drop in an R value of 0.017 with the addition of 540 anisotropic thermal parameters had a considerably less than 50% chance of being physically significant.

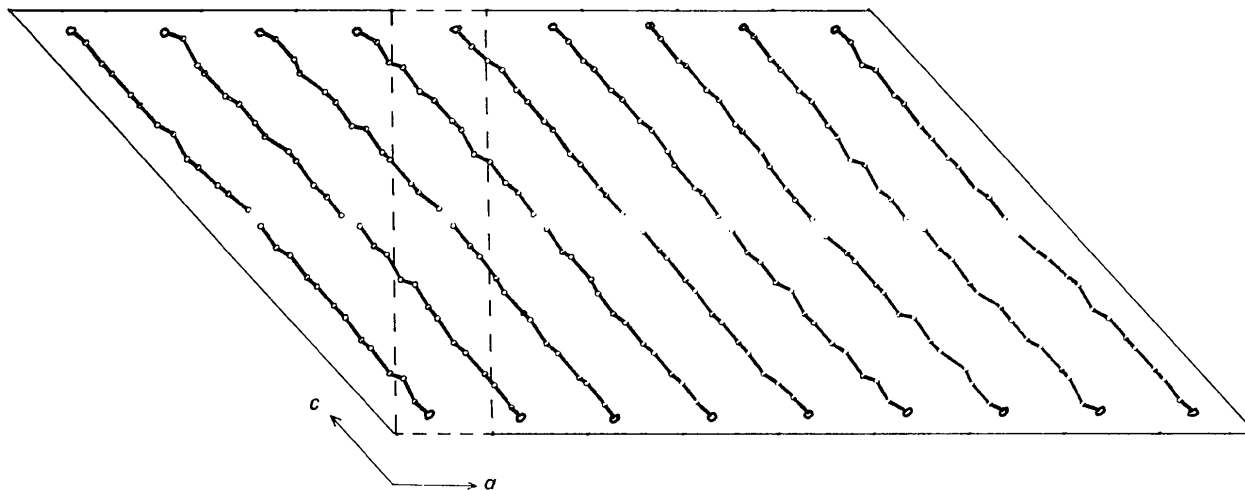


Fig. 3. A drawing of the subcell and true cell in direct space. The subcell is denoted by dashed lines. The nine molecules of the upper row are related to those of the lower by the twofold axis perpendicular to the plane of the drawing and located at $(a/2, c/2)$.

Results and discussion

A cell within a cell

The relationship between the true cell and the subcell in direct space is shown in Fig. 3. The true unit cell contains a basic pattern of a pair of hydrogen-bonded BUOL molecules whose coordinates are nearly the same as those of its neighbors, appropriately translated, but systematically different enough so that nine such pairs must occur before the arrangement truly repeats itself. Though the two-molecule unit, or subcell, manifests itself quite prominently in the diffraction pattern of the larger cell, considerable intensity

is present in non-subcell reflections because of deviations from subcell symmetry (primarily in the y coordinates of the atoms). Bond lengths and angles for the smaller cell are given in Table 8.

Packing in the b direction and hydrogen bonding are similar enough in both unit cells to be adequately represented by Fig. 4. Molecules pack in infinite sheets with an alternation of molecular tilt, approximately 27° to the ac plane, occurring from chain to chain. The literature contains no similar examples occurring in crystals of long-chain alcohols. Tilt alteration of entire double layers has been reported for certain monoglycerides (Larsson, 1964a), the D -polymorph of

Table 7. Final anisotropic thermal parameters of the nine bromine atoms of the asymmetric unit of the BUOL true cell

E.s.d.'s are in parentheses. All anisotropic values are multiplied by 10^4 and are defined by the expression:

$$\exp [-(B_{11}h^2 + B_{22}k^2 + B_{33}l^2 + B_{12}hk + B_{13}hl + B_{23}kl)]$$

	B_{11}	B_{22}	B_{33}	B_{12}	B_{13}	B_{23}
Br(1)	26 (2)	313 (79)	46 (5)	-7 (3)	54 (7)	3 (21)
Br(2)	30 (3)	453 (87)	44 (5)	0 (3)	59 (7)	-4 (17)
Br(3)	27 (2)	362 (69)	29 (4)	13 (3)	47 (6)	4 (13)
Br(4)	14 (1)	526 (89)	25 (3)	16 (3)	27 (5)	17 (17)
Br(5)	24 (2)	227 (73)	55 (5)	20 (4)	53 (6)	8 (21)
Br(6)	28 (2)	109 (77)	56 (5)	39 (4)	60 (7)	24 (18)
Br(7)	28 (2)	100 (63)	53 (6)	24 (3)	63 (7)	30 (14)
Br(8)	22 (2)	314 (77)	37 (4)	7 (4)	42 (6)	4 (16)
Br(9)	25 (2)	283 (71)	36 (4)	-9 (3)	50 (6)	-4 (18)

Table 8. Interatomic distances and angles in the BUOL subcell

A comparison of bond distances and bond angles within the BUOL subcell and the averaged values over all like-bonds and angles in the true cell. Quantities in parentheses are standard deviations, $[\sum(x-\bar{x})^2/n]^{1/2}$, and range value (in $\text{\AA} \times 100$ and degrees).

Br—C(11)	2.09 \AA	2.02 (5,17)	Br—C(11)—C(10)	107°	107 (7,21)
C(11)—C(10)	1.58	1.51 (9,17)	C(11)—C(10)—C(9)	108	108 (6,17)
C(10)—C(9)	1.50	1.53 (7,20)	C(10)—C(9)—C(8)	103	112 (7,18)
C(9)—C(8)	1.59	1.56 (10,30)	C(9)—C(8)—C(7)	102	113 (7,23)
C(8)—C(7)	1.56	1.61 (8,25)	C(8)—C(7)—C(6)	111	112 (6,18)
C(7)—C(6)	1.60	1.51 (7,21)	C(7)—C(6)—C(5)	112	107 (5,15)
C(6)—C(5)	1.48	1.61 (11,30)	C(6)—C(5)—C(4)	113	106 (4,16)
C(5)—C(4)	1.54	1.52 (5,16)	C(5)—C(4)—C(3)	117	109 (6,16)
C(4)—C(3)	1.36	1.53 (6,18)	C(4)—C(3)—C(2)	118	112 (8,27)
C(3)—C(2)	1.55	1.54 (13,38)	C(3)—C(2)—C(1)	111	110 (5,16)
C(2)—C(1)	1.56	1.60 (9,27)	C(2)—C(1)—O	108	107 (7,21)
C(1)—O	1.45	1.41 (8,25)	C—C—C	111° (5,16)	110 (6,27)
C—C	1.53 \AA (5,24)	1.55 (9,38)			

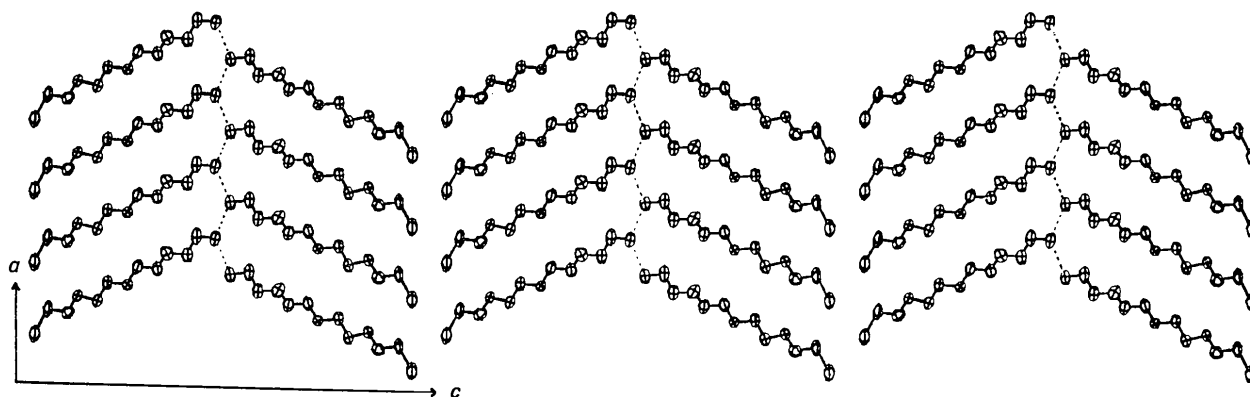


Fig. 4 A drawing of the hydrogen bonding scheme in BUOL. Hydrogen bonds are represented by dashed lines.

11-bromoundecanoic acid (Larsson, 1963) and methyl stearate (MacGillavry & Wolthuis-Spuy, 1970).

Hydrogen bonding

Every oxygen atom is hydrogen bonded to two others which are related by a twofold screw axis (in the subcell). The arrangement within the true cell is quite similar, except the symmetry element relating these pairs of molecules is a pseudo-twofold screw axis. Within each repeating double layer of molecules an infinite zigzag of hydrogen bonds, running in the *b* direction, exists. The oxygen-oxygen hydrogen bonded distance is 2.85 Å in the subcell. The five independent hydrogen bonds of the true cell vary from 2.70 to 3.00 Å but average 2.85 Å.

Planarity

The BUOL molecule appears to be essentially planar. However, when the deviations of every atom from a least-squares plane are averaged on an equivalent-atom basis over the nine independent molecules of the large cell, a slight curvature is found. These out-of-plane distances are given in Table 9. Deviations are small when compared to the uncertainty in atomic positions, and the pattern is not as prominent in the subcell.

Table 9. Deviation from planarity of the atoms in BUOL

A comparison of deviations within the BOUL subcell and deviations averaged over all the molecules of the true cell. The equation of the least-squares plane drawn through the 13 atoms of the BOUL subcell molecule is given by: $4.043x + 0.794y + 14.063z = 10.135$ Å, where *x*, *y*, and *z* are fractions of the subcell edges.

	Subcell	True cell
Br	-0.004 Å	0.068 Å
C(11)	0.058	0.063
C(10)	0.049	-0.005
C(9)	-0.026	-0.017
C(8)	-0.060	-0.045
C(7)	-0.050	-0.046
C(6)	0.011	-0.038
C(5)	-0.047	-0.086
C(4)	0.020	-0.042
C(3)	0.015	0.033
C(2)	0.007	0.005
C(1)	0.030	0.082
O	-0.002	0.046

Sinusoidal packing

Subtle differences exist between the packing schemes of the subcell and the true cell. Fig. 5 is a projection of the bromine positions onto the *ab* plane which reproduces the sinusoidal variation in the *y* coordinates of these nine atoms. The vertical scale has been magnified eightfold, and the horizontal line represents the average *y* coordinates of the bromine atoms. The amplitude of the displacement is ± 0.50 Å. When the *x* and *z* coordinates of these atoms are similarly plotted, they display a comparable sinusoidal arrangement with an amplitude of ± 0.17 Å.

The two orthogonal displacements are equivalent to an ellipsoidal helix with a pitch of 47.1 Å, the length of the *a* axis. A projection down this axis shows an ellipse with major and minor axes of 1.00 and 0.34 Å. The larger sinusoidal variation in the *y* coordinates is clearly present at every position in the aliphatic chain. However, the uncertainty in light-atom coordinates tends to obscure the smaller periodic displacement in *z* between equivalent atoms in neighboring chains. As a result, it is not possible to say whether the helical configuration undergoes any systematic distortion as one proceeds along the chain direction. The immediate environment of each of the nine molecules of the asymmetric unit differs slightly from that of its neighbors. This can be seen in Fig. 6, a schematic drawing of the packing between the planes of terminal bromine atoms.

Packing forces

A comparison of molecular arrangements within the two cells casts some light on why the larger cell is favored at room temperature. Such considerations require a close scrutiny of the two categories of molecular

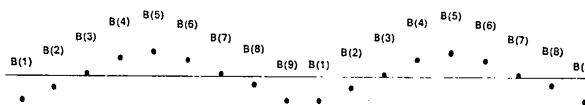


Fig. 5. Sinusoidal variation in the *y* coordinates of the nine independent bromine atoms in BUOL projected onto the *ab* plane. The average *y* coordinates of these atoms are represented by a line drawn parallel to the *a* axis. The deviation has been magnified eightfold.

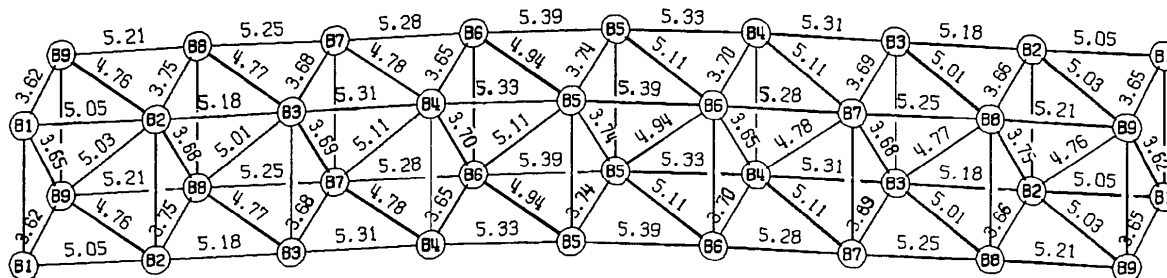


Fig. 6. Packing distances across the plane of bromine end groups. All vertical lines between bromine atoms are the length of one unit-cell translation in the *b* direction (5.26 Å).

interaction: chain packing and bromine end-group interaction.

Considering only the coordinates of the BUOL subcell, which represent an averaging of the contents of the true cell, chain packing may be more conveniently dealt with if the polymethylene subcell is considered. When this subcell, which represents the volume occupied by two $-\text{CH}_2-$ groups in a repeating array, is extracted from the present structure it is of the usual triclinic parallel type with dimensions $a_s=4.50$ (9), $b_s=5.26$ (0), $c_s=2.52$ (4) Å, $\alpha_s=64$ (2), $\beta_s=114$ (1), $\gamma_s=118$ (1)°, and $V_s=45.6$ (8) Å³. The relatively large size of this subcell suggests that packing of the hydrocarbon chain is not a contributing factor in determining the supercell structure.

A comparison of the van der Waals interaction energy at the bromine end-group interface distinguishes between the two arrangements. The relative contributions of the bromine–bromine, bromine–carbon, and carbon–carbon attractive interactions were evaluated using $U(R)=-\sum_j K_i(\sum_j R_{ij}^{-6})$, where K_i is a constant related to the electronic polarizability and instantaneous dipole moment of the atomic species involved (Kittel, 1967), and R_{ij} is the distance in Å separating the j th pair of atoms of interactions species i . Assuming the increase in repulsive terms (neglected in the previous formulation) to be minor (Larsson, 1964a), the summation of van der Waals interactions shows that the bromine–bromine interaction of the true cell is 30% greater than that found in the subcell. The other types of interaction differed by 3% at the most.

A comparison with other alcohols

While bromine can occasionally replace a terminal methyl group in an isomorphous manner (Larsson, 1963, 1964b), neither true cell nor subcell is isomorphous with any reported form of dodecanol. Studies of the higher alcohols have shown that dodecanol exists in two forms. The first, designated α in the nomenclature of Tanaka *et al.* (1959), occurs just below the melting point (23°C) and exhibits hexagonal symmetry usually associated with long-chain molecules possessing sufficient thermal energy to rotate about their long axes. The β form, a lower-melting polymorph, crystallizes in a monoclinic unit cell whose dimensions derived from powder photographs are radically different from either BUOL arrangement (Tanaka *et al.*, 1959). Tanaka *et al.* reported the molecular chains in this form to be perpendicular to the planes of their end groups, with each repeating layer two molecules in thickness.

A γ form has been reported for even-numbered long-chain alcohols having 16 or more carbon atoms (Watanabe, 1961). The long chains in this form are indeed tilted 55° with respect to their plane of end groups, but there is no alternation of tilt as in BUOL.

The structure of hexadecanol as determined by Abrahamsson *et al.* (1960) showed a radically different hydrogen bonding scheme, with bonds occurring across centers of symmetry and twofold axes. While there are eight molecules in this particular unit cell, it is a consequence of a face-centered monoclinic cell rather than a subcell.

In BUOL, with only 11 carbon atoms in its chain, the presence of an electron-rich bromine atom is most likely the determining factor in the overall structure of the repeating unit. Attraction between planes of bromine atoms probably accounts for the 23°C rise in melting-point temperature, and it plays a critical role in 'deciding' why it is energetically more favorable for BUOL molecules to assume the alternating tilt and sinusoidal packing of the supercell arrangement.

Research in this study was supported by grants GM-12376 and HE-11914 from the National Institutes of Health. Author L.R. was supported by a predoctoral fellowship from NIGMS (5-FI-GM-31709) and a graduate training grant from NIH (GM-719). Computer time was supported in part by a NASA grant (NsG 398) to the Computer Science Center of the University of Maryland.

References

- ABRAHAMSSON, S., LARSSON, G., & VON SYDOW, E. (1960). *Acta Cryst.* **13**, 770.
- ALEXANDER, L. E. & SMITH, G. S. (1962). *Acta Cryst.* **15**, 983.
- HAMILTON, W. D. (1965). *Acta Cryst.* **18**, 502.
- International Tables for X-ray Crystallography* (1962). Vol. III, p. 202–207, p. 215. Birmingham: Kynoch Press.
- JOHNSON, C. K. (1965). *ORTEP, A Fortran Thermal Ellipsoid Plot Program for Crystal Structure Illustration*. Report ORNL-3794. Rev. Ed. Oak Ridge National Laboratory, Oak Ridge, Tennessee.
- KITTEL, C. (1967). *Introduction to Solid State Physics*, 3rd Ed. New York: John Wiley.
- KOLB, D. G. & LUTTON, E. S. (1951). *J. Amer. Chem. Soc.* **73**, 5593.
- LARSSON, K. (1963). *Acta Chemica Scand.* **17**, 199.
- LARSSON, K. (1964a). *Ark. Kemi*, **23**, 29.
- LARSSON, K. (1964b). *Ark. Kemi*, **23**, 1.
- MACGILLAVRY, C. H. & WALTHUIS-SPUY, M. (1970). *Acta Cryst.* **B26**, 645.
- MALKIN, T. (1930). *J. Amer. Chem. Soc.* **52**, 3739.
- STOUT, G. H. & JENSEN, L. H. (1968). *X-ray Structure Determination*, p. 161. New York: Macmillan.
- TANAKA, K., SETO, T. & HAYASHIDA, T. (1957). *Bull. Inst. for Chemical Research (Kyoto Univ.)*, **35**, 123.
- TANAKA, K., SETO, T., WATANABE, A. & HAYASHIDA, T. (1959). *Bull. Inst. for Chemical Research (Kyoto Univ.)*, **35**, 281.
- WATANABE, A. (1961). *Bull. Chem. Soc. Japan*, **34**, 1728.
- WATANABE, A. (1962). *Bull. Chem. Soc. Japan*, **36**, 336.
- WELSH, H. K. (1956). *Acta Cryst.* **9**, 89.
- WELSH, H. K. (1960). *Acta Cryst.* **13**, 770.